# CHAPTER 4 RESULTS AND DISCUSSION

The series of lead borate glasses prepared in composition (100-x)$B_2O_3$ : xPbO (where x is 30, 40, 50, 60 and 70 wt%) using a conventional melt quenching technique. Chemical powers of analytical reagent consisted of PbO (UNILAB, 99.99%) and $H_3BO_3$ (UNIVAR, 99.99 %). All chemical composition was finely powder and then mixed in whole of composite. Batches for producing 30 g of glass were melted in alumina crucibles in an electric furnace at 1100°C with soaking time for 3 hours under normal atmospheric conditions. Afterwards, the melts were quickly poured onto a preheated stainless steel plate and pressed to a thickness of approximately 0.5 mm by another plate, annealed at 500°C for 3 hours, and slowly cooled down to room temperature, respectively. Finally, the as-prepared glass samples were cut and then finely polished to a dimension of 1.0 cm x 2.0 cm x 0.3 cm. The chemical compositions of $B_2O_3$-PbO glasses prepared in the present study are given in Table 4.1. The homogeneous glass samples for all compositions of lead borate are optically transparent and are illustrated in Figure. 4.1. The intensity of yellow color of glasses was increased with increasing PbO content.

**Table 4.1** The chemical compositions of the as-prepared glasses.

| Sample No. | PbO (wt %) | Glass composition (wt%) |
|---|---|---|
| 1 | 30 | 30PbO : 70$B_2O_3$ |
| 2 | 40 | 40PbO : 60$B_2O_3$ |
| 3 | 50 | 50PbO : 50$B_2O_3$ |
| 4 | 60 | 60PbO : 40$B_2O_3$ |
| 5 | 70 | 70PbO : 30$B_2O_3$ |

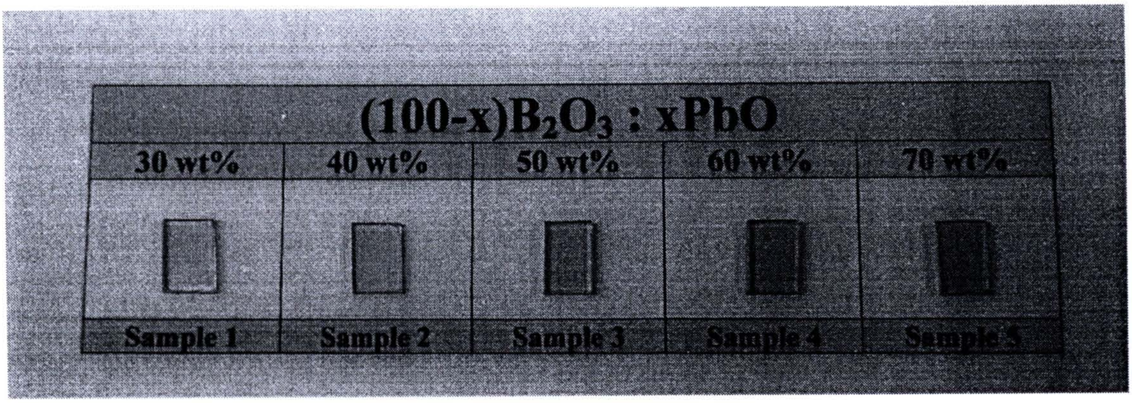


**Figure 4.1** Photographs of the as-prepared glass samples.

## 4.1 Density and Molar Volume

The determined density ($\rho$), molar volume ($V_M$) of lead borate glass samples for different PbO concentrations are given in Table 4.2. The variations of the density and molar volume are the function of PbO content and are also shown in Figure. 4.2 and Figure 4.3, respectively. As can be seen from Figure 4.2, the density indicates that replacing $B_2O_3$ by addition of some amount of PbO results in the increase of the average molecular weight of oxide ions in the glass due to PbO has a higher relative molecular weight than that of $B_2O_3$.

Based on the measured density, the molar volume can be determined and can be explained in term of non-bridging oxygen (NBOs). In this study, when the PbO content less than 40 wt%, entered PbO may act as a network former, so molar volume of glass decreased. Beyond 40 wt%, interactomic spacing increased due to more ionic bond are created and generated more NBOs in borate network due to PbO act as modifier. Then molar volume were increased.

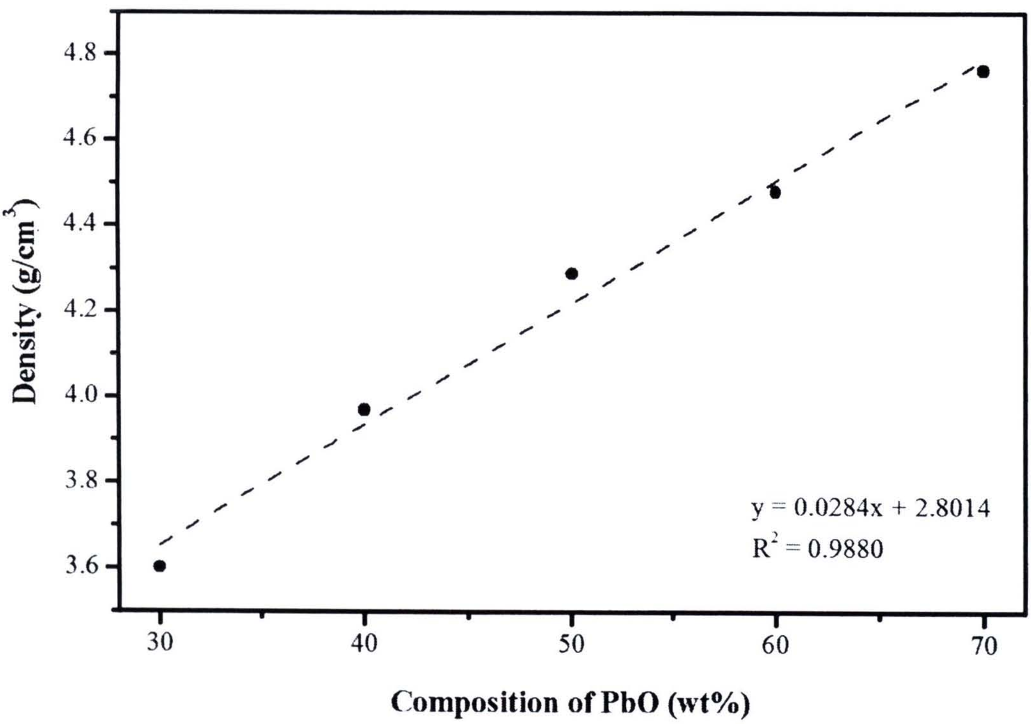


**Figure 4.2** The density of glass samples as a function of PbO content in borate glasses.

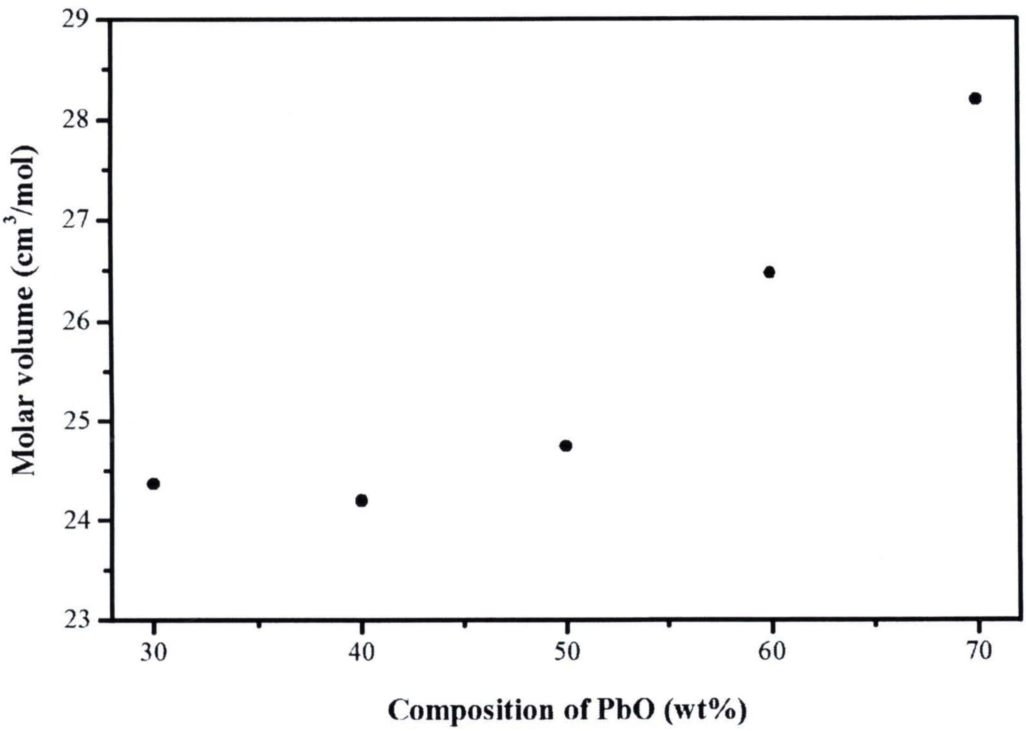


**Figure 4.3** The molar volume of glass samples as a function of with PbO content in borate glasses.

**Table 4.2** The values of density ($\rho$), molecular weight ($M_T$) and molar volume ($V_M$) of glass samples.

| Sample No. | Glass formula wt% | Density $\rho$ (g/cm$^3$) | Molecular weight $M_T$ (g/mol) | Molar volume $V_M$ (cm$^3$/mol) |
|---|---|---|---|---|
| 1 | $30PbO : 70B_2O_3$ | 3.6003±0.0018 | 87.73 | 24.37 |
| 2 | $40PbO : 60B_2O_3$ | 3.9700±0.0034 | 96.05 | 24.19 |
| 3 | $50PbO : 50B_2O_3$ | 4.2898±0.0079 | 106.14 | 24.74 |
| 4 | $60PbO : 40B_2O_3$ | 4.4794±0.0084 | 118.57 | 26.47 |
| 5 | $70PbO : 30B_2O_3$ | 4.7651±0.0073 | 134.31 | 28.19 |

## 4.2 UV-Visible Absorption Study

The optical absorption spectra at room temperature for the equal thickness glasses were measured covering the wavelength 190-1100 nm using UV-Visible spectrophotometer (Cary-50, Varian).

The cutoff wavelength ($\lambda_{cutoff}$) position of the spectra, the wavelength at which the percentage transmission is zero, tends to shift slightly towards longer wavelength with as the content of PbO increase and the corresponding color of lead borate glass (stronger yellow) is shown in Figure 4.1.

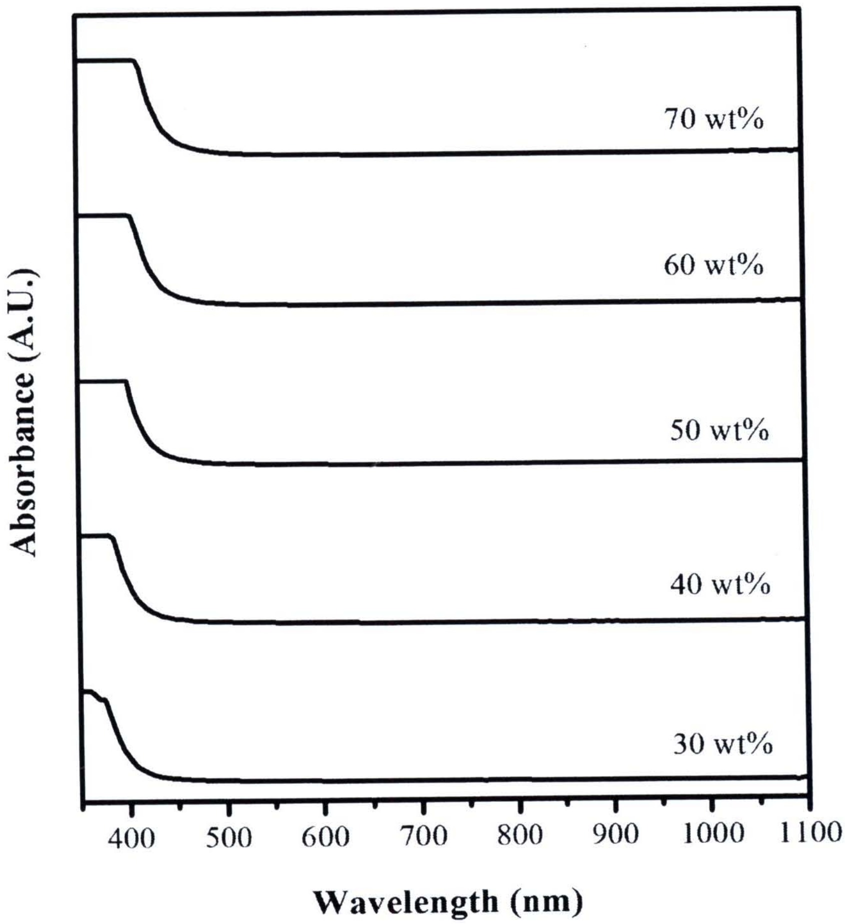


**Figure 4.4** The absorption spectra of lead borate glass samples.

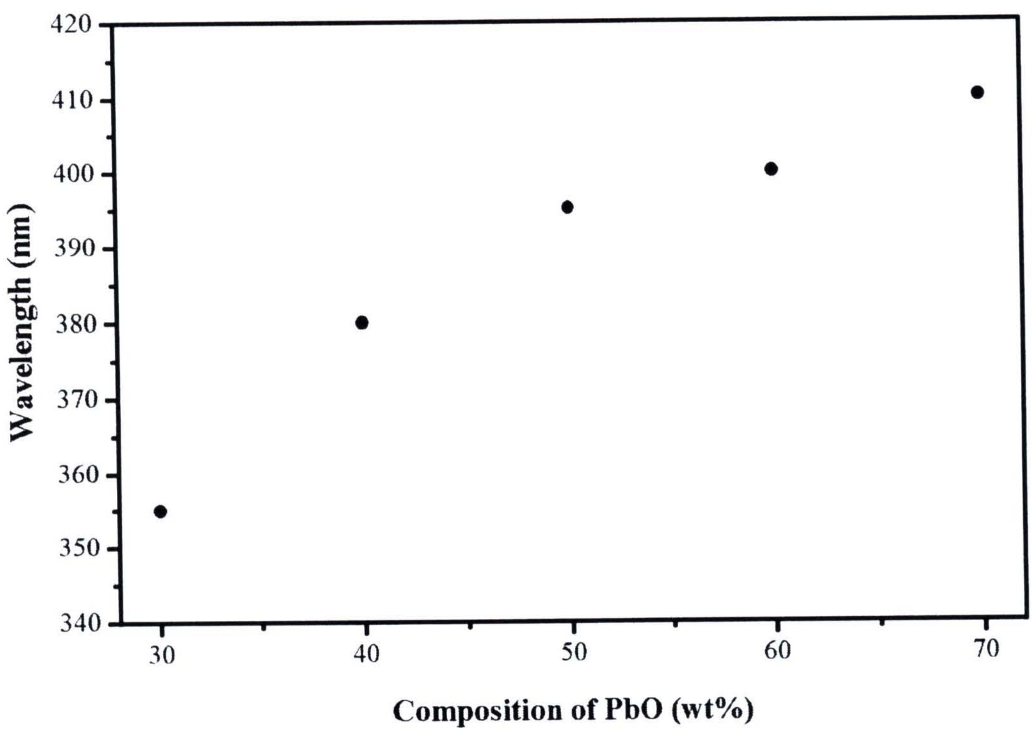


**Figure 4.5** The cuttoff wavelength of lead borate glass samples.

**Table 4.3** The cutoff wavelength ($\lambda_{cutoff}$) for all glass samples.

| Composition (wt%) | | Glass formula (wt%) | $\lambda_{cutoff}$ (nm) |
|---|---|---|---|
| PbO | $B_2O_3$ | | |
| 30 | 70 | $30PbO : 70B_2O_3$ | 355 |
| 40 | 60 | $40PbO : 60B_2O_3$ | 380 |
| 50 | 50 | $50PbO : 50B_2O_3$ | 395 |
| 60 | 40 | $60PbO : 40B_2O_3$ | 400 |
| 70 | 30 | $70PbO : 30B_2O_3$ | 410 |

## 4.3 Optical Band Gap and Refractive Index [72]

The optical absorption at the fundamental edge, where $\alpha \geq 10^4$, in terms of the theory was interpreted by Davis and Mott [72] and can be written in general form;

$$\alpha h(\nu) = B^2(h\nu - E_g)^r \tag{4.2}$$

where $B$ is a constant called the band tailing parameter, $h\nu$ is the incident photon energy, $E_g$ is optical band gap and paramenter $r$ is the index which can be different values such as 2, 3, 1/2 and 1/3 which corresponding to indirect allowed, indirect forbidden, direct allowed and direct forbidden transitions, respectively.

The absorption coefficients, $\alpha(v)$, were determined near the absorption edge of different photon energies for all glass samples. It is well-known that for amorphous materials, a reasonable fit of Eq. (4.2) with $n = 2$ are achieved. Therefore, the typical plot of $(\alpha hv)^{1/2}$ versus photon energies ($hv$) (Tauc's plot), for indirect allowed transitions to find the values of optical band gap, ($E_g$) is shown in Figure 4.6. It can be seen that there exists a linear dependence of $(\alpha hv)^{1/2}$ to the photon energy. This suggests that at higher photon energies, the transitions occurring in the glass samples are of indirect type. The obtained values of $E_g$ are listed in Table 4.4.

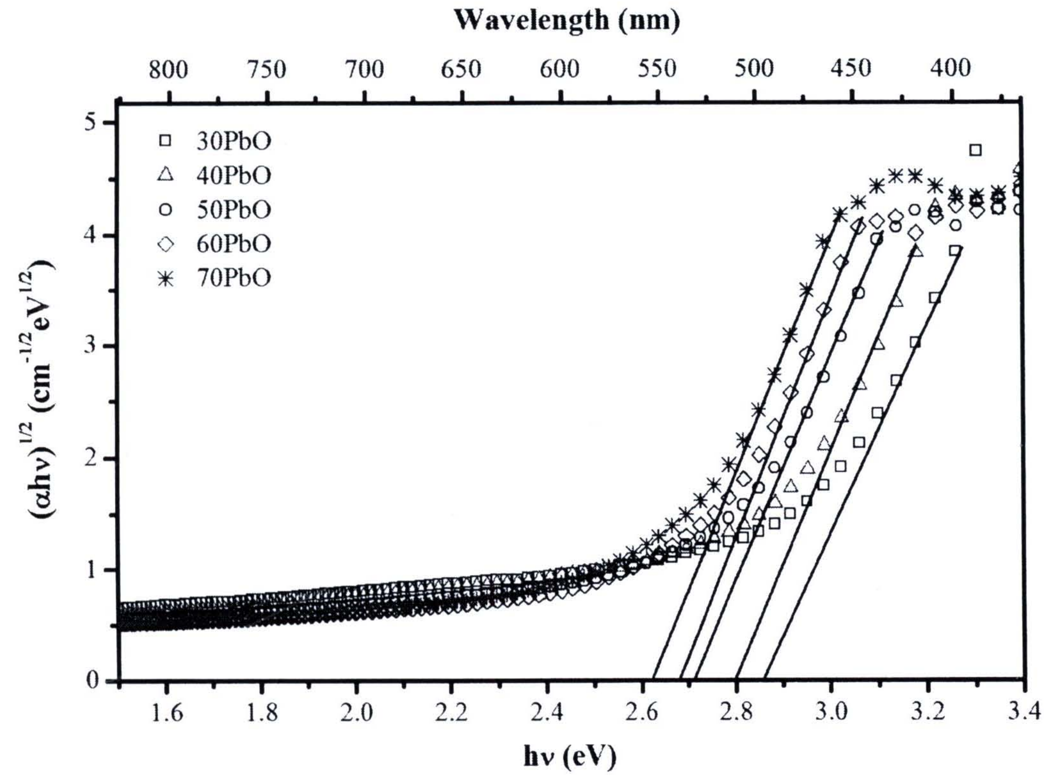


**Figure 4.6** The absorption extrapolation of Tauc's plot of lead borate samples.

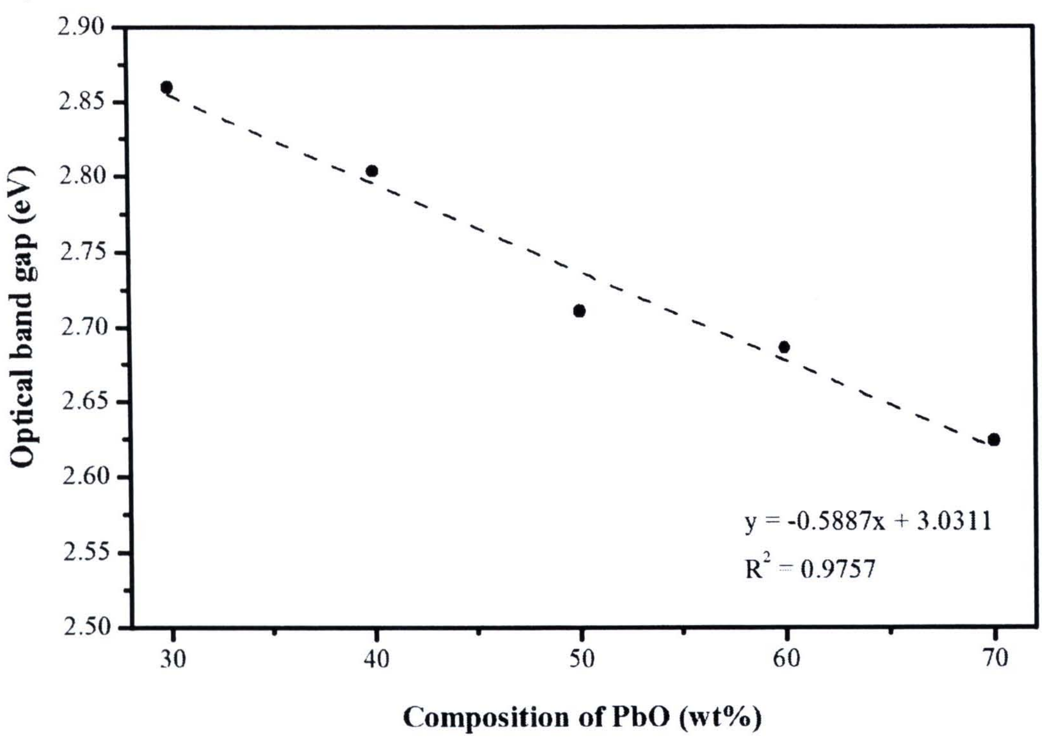


**Figure 4.7** The variations of optical band gap values of the glasses over the PbO concentration.

From the band theory view, the addition of PbO concentration in all glass samples results in the slightly decrease in the optical band gap and shift the absorption edge to the longer wavelength.

Refractive index is one of the important properties in optical glasses. Therefore, a large number of researchers have carried out investigations to ascertain the relation between refractive index and glass composition. The refractive index of all research glasses, cannot be evaluated by using refractometer According to Dimitrov [47-49], the refractive index has been calculated using the following relation;

$$\frac{(n^2-1)}{(n^2+2)} = 1 - \sqrt{\frac{E_g}{20}} \quad (4.3)$$

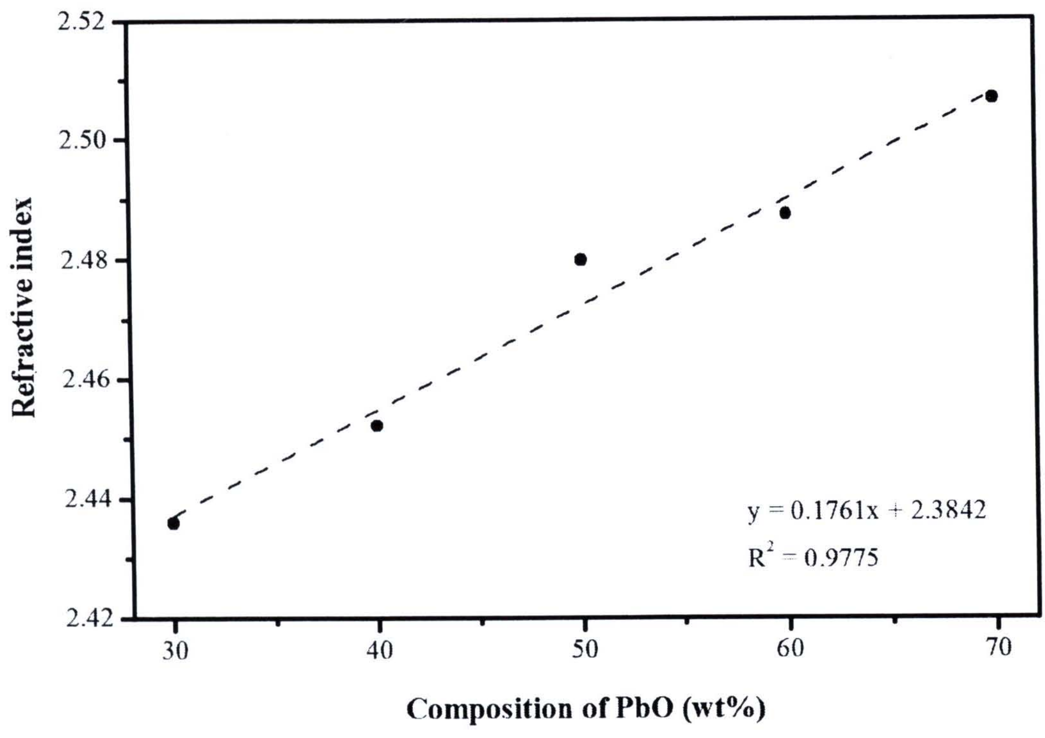


**Figure 4.8** The variation of refractive index values over the PbO concentration.

Refractive index is one of the important properties in optical glasses. Therefore, a large number of researchers have carried out investigations to a certain the relation between refractive index and glass composition. By using Eq. (4.3), the refractive index of all research glasses was obtained. As can be seen in Figure 4.8, the refractive index of the glasses decreases gradually with increasing the concentration of PbO.

**Table 4.4** The optical band gap ($E_g$) and refractive index ($n$) for all glass samples.

| Composition (wt%) | | Glass formula (wt%) | $E_g$ (eV) | $n$ |
|---|---|---|---|---|
| PbO | $B_2O_3$ | | | |
| 30 | 70 | $30PbO : 70B_2O_3$ | 2.86 | 2.44 |
| 40 | 60 | $40PbO : 60B_2O_3$ | 2.80 | 2.45 |
| 50 | 50 | $50PbO : 50B_2O_3$ | 2.71 | 2.48 |
| 60 | 40 | $60PbO : 40B_2O_3$ | 2.69 | 2.49 |
| 70 | 30 | $70PbO : 30B_2O_3$ | 2.62 | 2.51 |

## 4.4 Optical Basicity

The optical basicity ($\Lambda$) of an oxidic medium is an express of the average electron donor power of all the oxide atoms constituting the medium. The optical basicity could be predicted from the glass compositions. Simultaneously, it is possible to calculate the so-called theoretical optical basicity $\Lambda_{th}$ which is based on the approach proposed by Duffy and Ingram [60-62].

$$\Lambda_{th} = x_{PbO}\Lambda_{PbO} + x_{B_2O_3}\Lambda_{B_2O_3} \tag{4.4}$$

where $x_{PbO}$ and $x_{B2O3}$ denote the equivalent fractions based on the amount of oxygen each oxide contributes to the overall stoichiometry and $\Lambda_{PbO}$ and $\Lambda_{B2O3}$ are basicities assigned to the individual oxide, these values are taken from Table 2.6.

**Table 4.5** The optical basicity of lead borate glass samples.

| Sample No. | Composition (wt%) | | Glass formula (wt%) | Optical basicity $\Lambda_{th}$ |
|---|---|---|---|---|
| | PbO | $B_2O_3$ | | |
| 1 | 30 | 70 | $30PbO : 70B_2O_3$ | 0.46 |
| 2 | 40 | 60 | $40PbO : 60B_2O_3$ | 0.48 |
| 3 | 50 | 50 | $50PbO : 50B_2O_3$ | 0.50 |
| 4 | 60 | 40 | $60PbO : 40B_2O_3$ | 0.53 |
| 5 | 70 | 30 | $70PbO : 30B_2O_3$ | 0.58 |

Increasing optical basicity of glasses with higher PbO concentration indicates the increasing of negative charges on the oxygen atoms and, thus, increasing covalency force in the cation-oxygen bonding. It is clearly observed from Figure 4.9 that the increase of optical basicity in this work means the higher ability of oxide ions to transfer electrons to the surrounding cations.

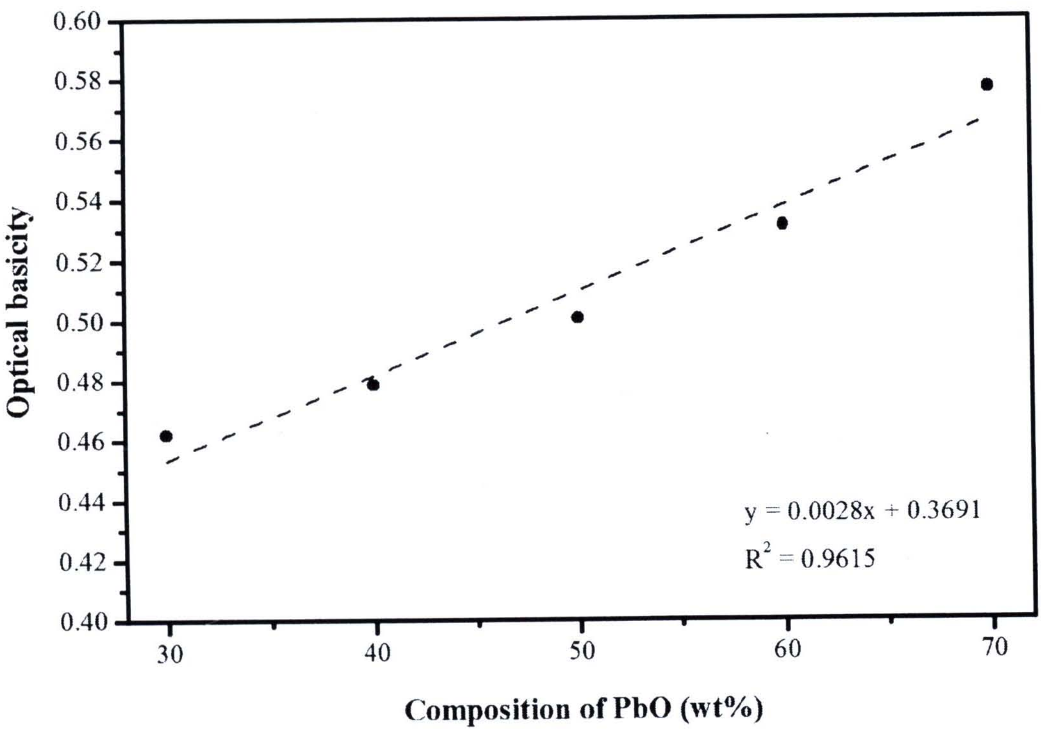


**Figure 4.9** The values of optical basicity of glass samples as a function of PbO content.

## 4.5 Gamma-Rays Shielding Properties

The mass attenuation coefficients ($\mu_m$) of research glasses are given in Table 4.6. According to the Gamma-ray transmission experiment, the experimental values of mass attenuation coefficient were obtained from the gamma-rays incidented ($I_0$) and transmitted ($I$) intensities and in order to get the theoretical values, WinxCom program was used. It has been found that the mass attenuation coefficients were increased with increasing of PbO content in glass system, indicates the better shielding properties. Also, the experimental values of mass attenuation coefficient are in good agreement with the theoretical values also shown graphically in Figure 4.10. The increase photon interaction probability at this photon energy leads to the decrease of gamma-rays transmission with increasing amount of PbO.

The data in Table 4.6 shown the relative different of mass attenuation coefficients were less than 1% reflecting the good detection system setup of transmission experiment. The value differences between experiment and theory suggested systematic errors; this may be due to non-stoichiometry ratio of glass formula after melting at high temperature.

**Table 4.6** The mass attenuation coefficients of $PbO-B_2O_3$ glass system at 662 keV.

| Sample No. | Composition (wt%) | | $\mu_{m(th)} \times 10^{-2}$ ($cm^2/g$) | $\mu_{m(ex)} \times 10^{-2}$ ($cm^2/g$) | %RD |
|---|---|---|---|---|---|
| | PbO | $B_2O_3$ | | | |
| 1 | 30 | 70 | 8.51 | 8.31 ± 0.18 | 0.01 |
| 2 | 40 | 60 | 8.84 | 8.93 ± 0.17 | 0.01 |
| 3 | 50 | 50 | 9.16 | 8.87 ± 0.10 | 0.03 |
| 4 | 60 | 40 | 9.48 | 9.12 ± 0.16 | 0.02 |
| 5 | 70 | 30 | 9.81 | 9.96 ± 0.14 | 0.01 |

* RD = Relative difference $\mu_m$ of between experiment and theory.

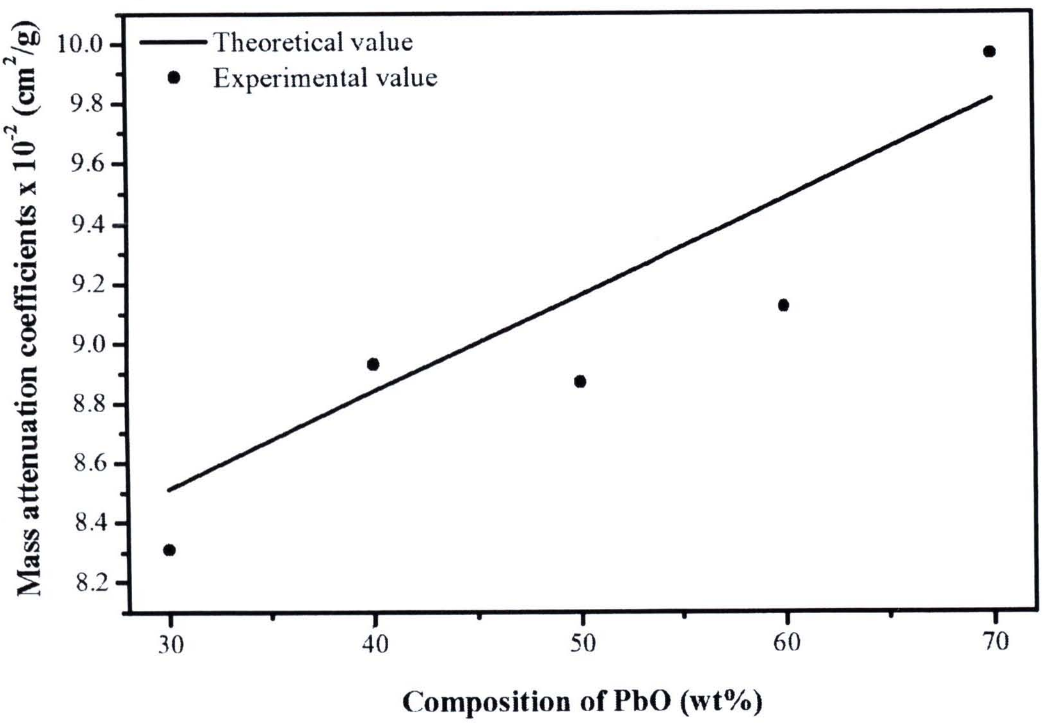


**Figure 4.10** The variation of theoretical values and experimental values of total mass attenuation coefficients at 662 keV as a function of PbO content.

It is clearly seen that the values of total mass attenuation coefficients depends on the PbO content of the studied glasses. With increasing of PbO concentration, the mass attenuation coefficients values increases which may be due to the increase in the weight fraction of the higher atomic number constituent element (Pb).

Furthermore, the behavior of the partial photon interactions in this energy also were studied using the WinXCom program and the results are shown graphically in Figure 4.11 - 4.13.

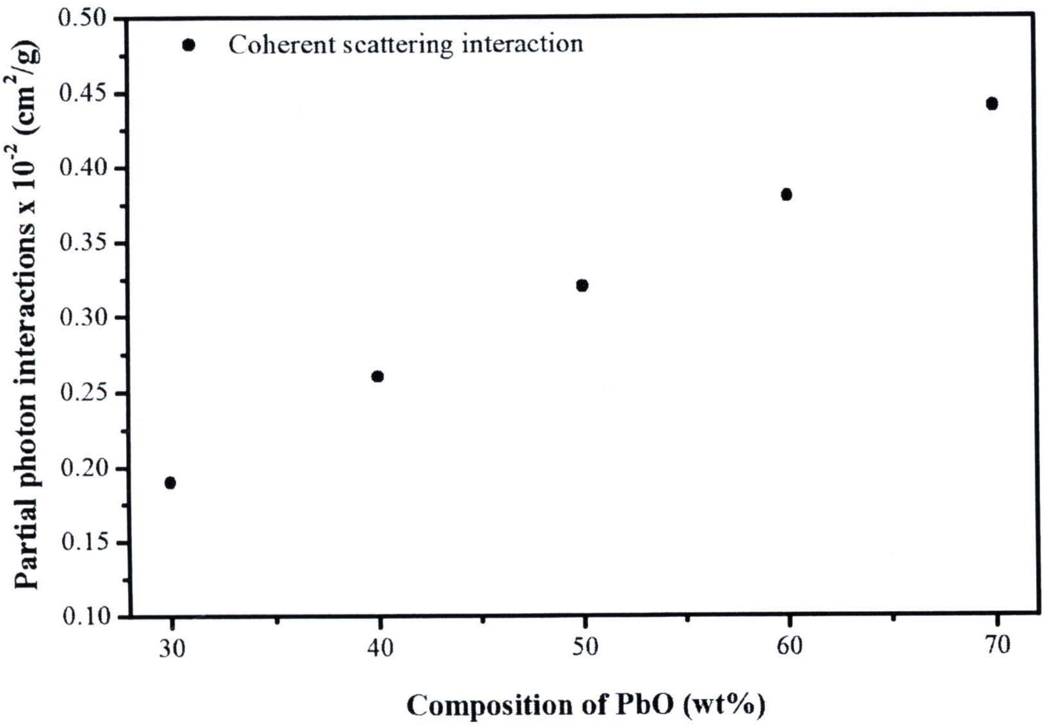


**Figure 4.11** The variation of coherent scattering interaction at 662 keV as a function of PbO content.

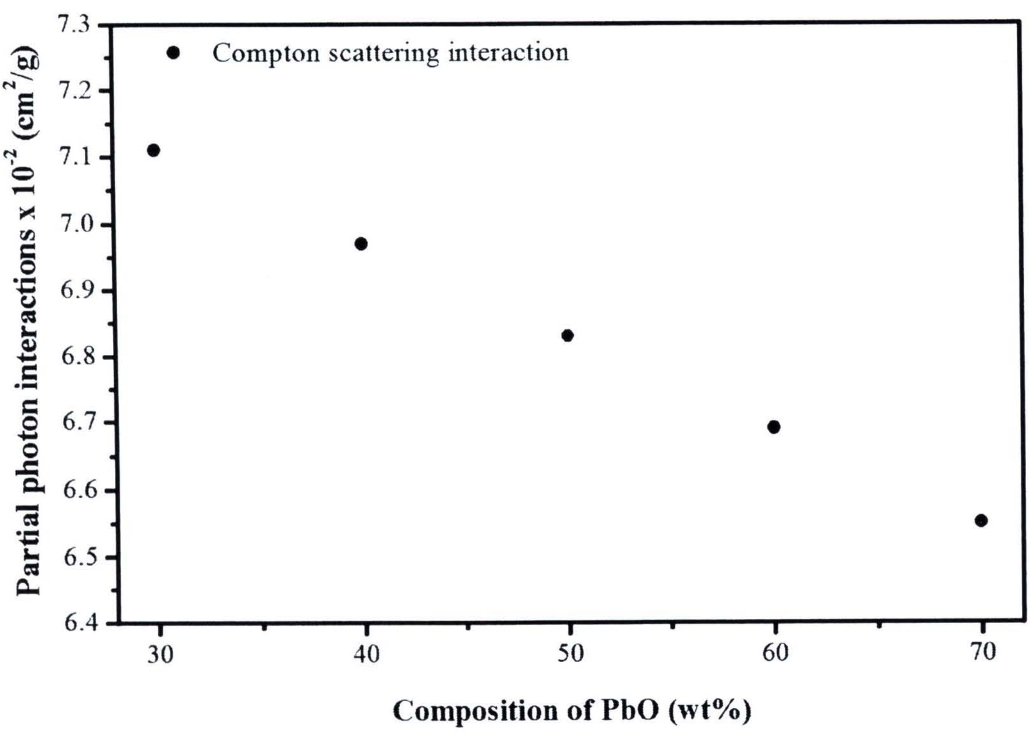


**Figure 4.12** The variation of Compton scattering interaction at 662 keV as a function of PbO content.

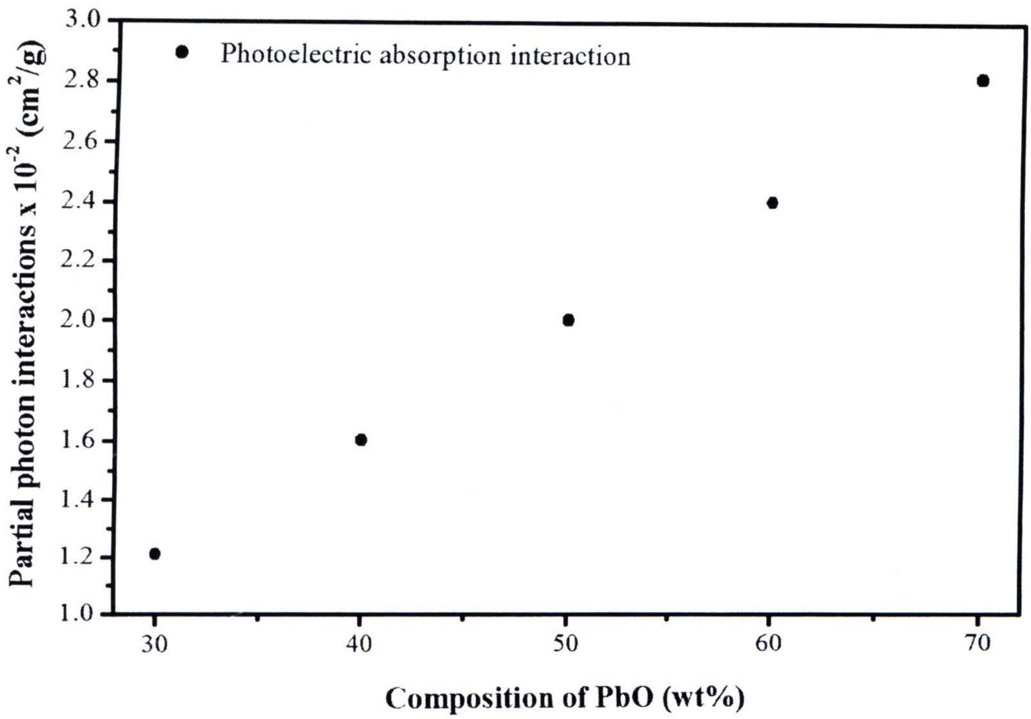


**Figure 4.13** The variations of photoelectric absorption interaction at 662 keV as a function of PbO content.

It is observed that the coherent scattering, incoherent scattering and photoelectric absorption processes changed with PbO content. For the photon energy less than 1.022 MeV, the pair production process is not occurred for all glasses.

In addition, the behaviour of total mass attenuation coefficients against the PbO content for each partial photon process has been studied (Figure 4.14).

**Table 4.7** The partial interactions of $PbO-B_2O_3$ glass system at 662 keV.

| Sample No. | $\mu_{m(ex)} \times 10^{-2}$ ($cm^2/g$) | Partial photon interactions × $10^{-2}$ ($cm^2/g$) | | | |
|---|---|---|---|---|---|
| | | Coherent | Compton | Photoelectric | Total |
| 1 | 8.31 ± 0.18 | 0.19 | 7.11 | 1.21 | 8.31 |
| 2 | 8.93 ± 0.17 | 0.26 | 6.97 | 1.61 | 8.93 |
| 3 | 8.87 ± 0.10 | 0.32 | 6.83 | 2.01 | 8.87 |
| 4 | 9.12 ± 0.16 | 0.38 | 6.69 | 2.41 | 9.12 |
| 5 | 9.96 ± 0.14 | 0.44 | 6.55 | 2.82 | 9.96 |

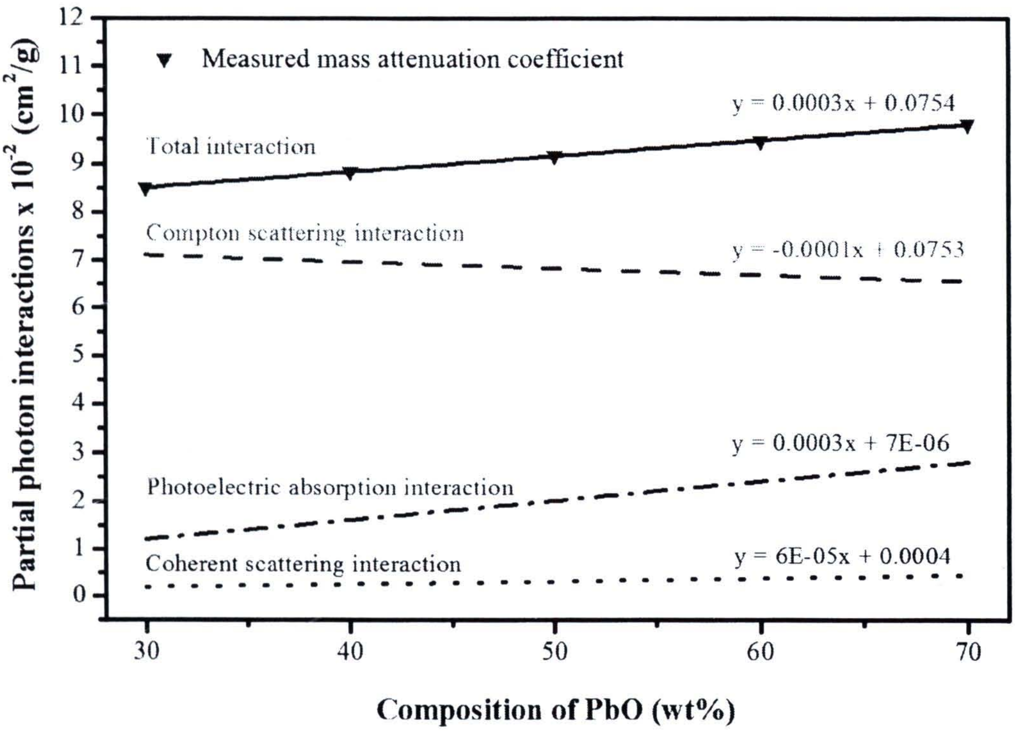


**Figure 4.14** Mass attenuation coefficients with partial interactions of $PbO$-$B_2O_3$ glass system at 662 keV.

It is clearly seen that the values of total mass attenuation coefficient were increased due to the increasing of photoelectric absorption at this energy. However, the Compton scattering is the dominant photon process.

According to the theoretical approach in Chapter 2 and the values of mass attenuation coefficients, another radiation shielding parameters such as total atomic cross-section ($\sigma_{t,a}$), total electronic cross-section ($\sigma_{t,el}$), effective atomic number ($Z_{eff}$) and effective electron density ($N_e$) were evaluated for $(100\text{-}x)B_2O_3$: $x$PbO glass system.

Among this, the effective atomic number ($Z_{eff}$) and effective electron density ($N_e$) have been determined using the Eq. (2.35) and Eq. (2.36), respectively, are enlisted in Table 4.9. In Figure 4.15 shows the good agreement between experimental values and theoretical values of total atomic cross-section.

**Table 4.8** The theoretical and experimental values of total atomic cross-section of $PbO$-$B_2O_3$ glass system at 662 keV.

| Sample No. | Glass formula (wt%) | $\sigma_{t,a(th)}$ (b/atom) | $\sigma_{t,a(ex)}$ (b/atom) |
|---|---|---|---|
| 1 | 30PbO : $70B_2O_3$ | 2.671 | 2.610 |
| 2 | 40PbO : $60B_2O_3$ | 3.145 | 3.180 |
| 3 | 50PbO : $50B_2O_3$ | 3.767 | 3.650 |
| 4 | 60PbO : $40B_2O_3$ | 4.620 | 4.440 |
| 5 | 70PbO : $30B_2O_3$ | 5.856 | 5.940 |

**Table 4.9** The theoretical and experimental values of effective atomic number and effective electron number of $PbO$-$B_2O_3$ glass system at 662 keV.

| Sample No. | Glass formula (wt%) | $Z_{eff(th)}$ ($e^-$/atom) | $Z_{eff(ex)}$ ($e^-$/atom) | $N_{e(th)} \times 10^{23}$ ($e^-$/g) | $N_{e(ex)} \times 10^{23}$ ($e^-$/g) |
|---|---|---|---|---|---|
| 1 | $30PbO : 70B_2O_3$ | 10.19 | 9.96 | 3.25 | 3.17 |
| 2 | $40PbO : 60B_2O_3$ | 11.35 | 12.01 | 3.34 | 3.37 |
| 3 | $50PbO : 50B_2O_3$ | 14.06 | 13.60 | 3.42 | 3.30 |
| 4 | $60PbO : 40B_2O_3$ | 16.92 | 16.28 | 3.48 | 3.34 |
| 5 | $70PbO : 30B_2O_3$ | 20.94 | 21.25 | 3.51 | 3.56 |

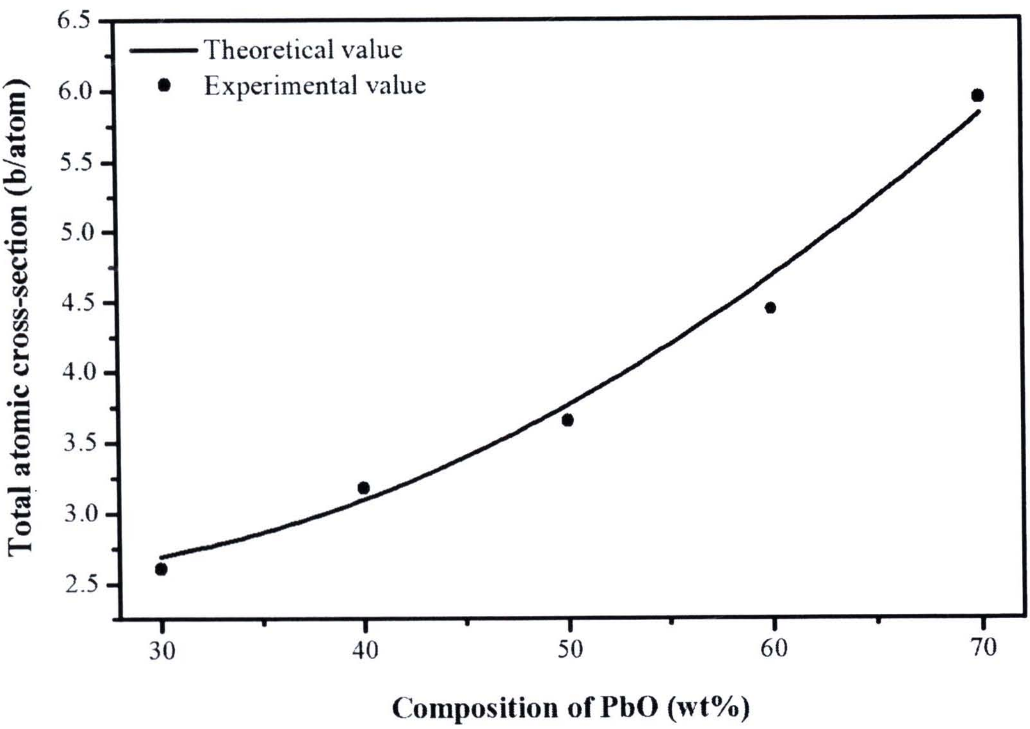


**Figure 4.15** Total atomic cross-sections at this photon energy of $PbO$-$B_2O_3$ glass system.

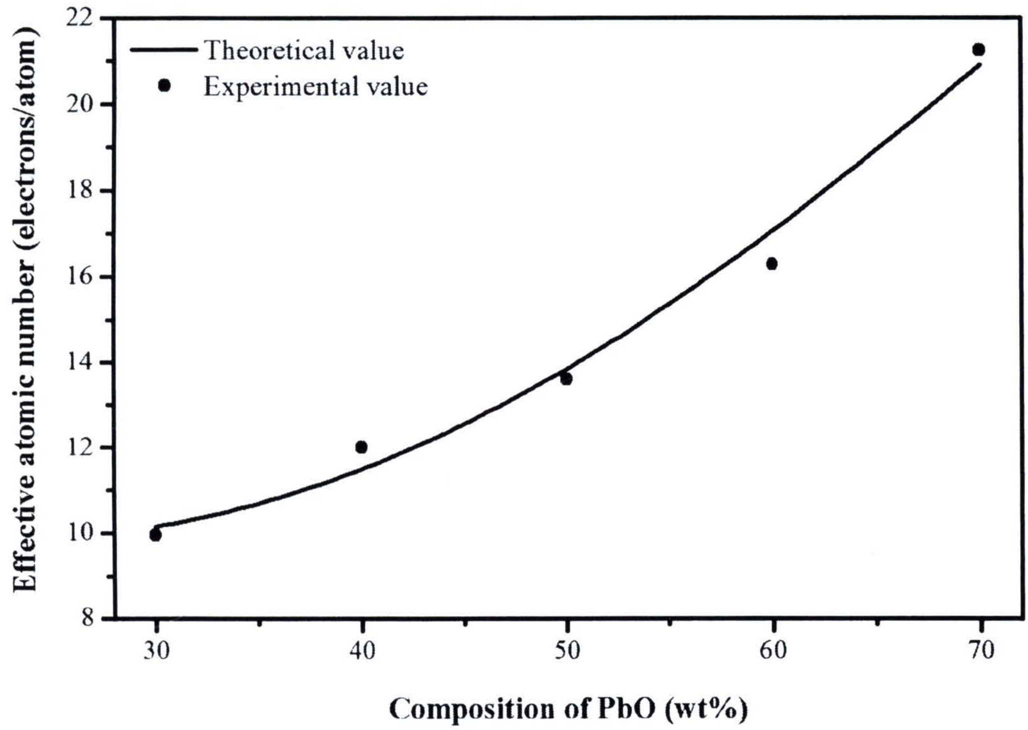


**Figure 4.16** Effective atomic numbers at photon energy 662 keV of $PbO\text{-}B_2O_3$ glass system.

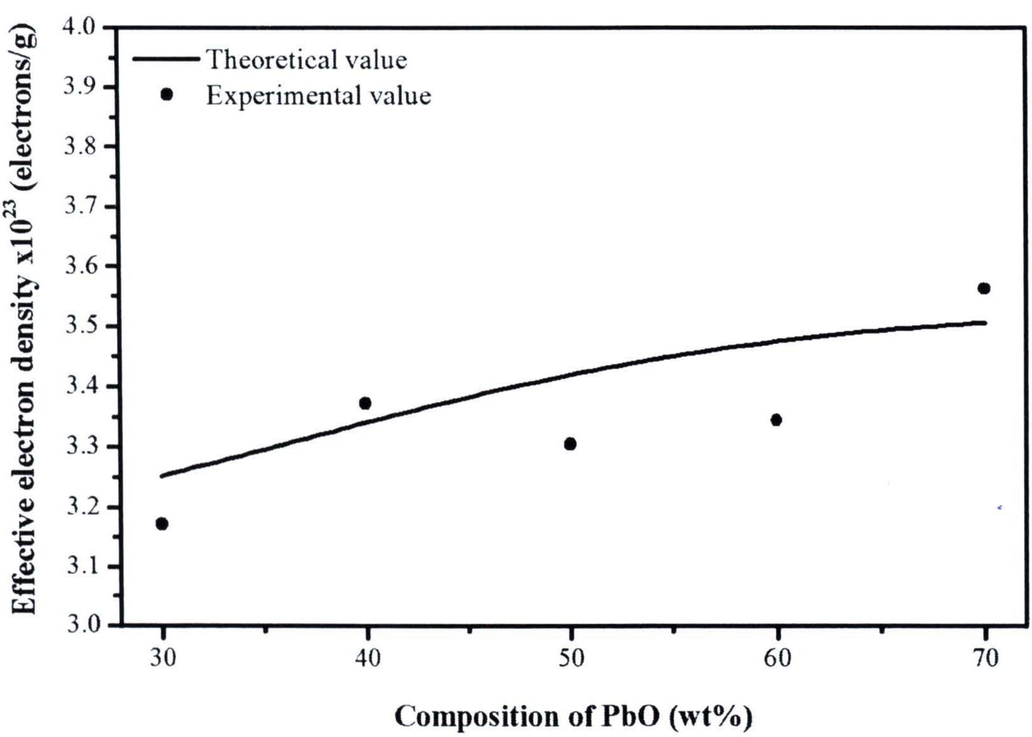


**Figure 4.17** Effective electron densities at photon energy 662 keV of $PbO\text{-}B_2O_3$ glass system.

As seen in Figure 4.16 and Figure 4.17, the experimental values of effective atomic number and effective electron density are the good agreement with the theoretical values. In addition, it is observed that the effective atomic numbers and effective electron densities were changed with higher PbO concentration for all glasses, corresponding to the increasing of mass attenuation coefficients. The dependence of the effective atomic number shows that lead borate glasses having high effective atomic numbers absorb effectively incoming photon.

Finally, the half value layer parameter (*HVL*) of the research glass samples has been evaluated and enlisted in Table 4.10. To compare the values of lead borate glasses with values of some standard shielding concretes, the density, chemical composition and linear attenuation coefficient of concretes have been taken from literature [2]. The obtained values of half value layer of literature [2] concretes were also shown in Table 4.11. Out of all concretes, the values of half value layer for ferrite concrete (or iron concrete) have been observed to be minimum. Hence, its value has been taken for comparison with the lead borate glasses and is shown in Figure 4.18.

**Table 4.10** The half value layer parameter of $PbO\text{-}B_2O_3$ glass system at 662 keV.

| Sample No. | Glass formula (wt%) | *HVL* (cm) |
|---|---|---|
| 1 | $30PbO : 70B_2O_3$ | 2.32 |
| 2 | $40PbO : 60B_2O_3$ | 1.95 |
| 3 | $50PbO : 50B_2O_3$ | 1.82 |
| 4 | $60PbO : 40B_2O_3$ | 1.70 |
| 5 | $70PbO : 30B_2O_3$ | 1.46 |

**Table 4.11** The half value layer parameter of some radiation shielding concretes [2] at 662 keV.

| Shielding Concretes | *HVL* (cm) |
|---|---|
| Ordinary | 3.87 |
| Barite | 2.54 |
| Ferrite (Iron concrete) | 1.98 |
| Chromite | 2.82 |
| Serpentine | 4.07 |

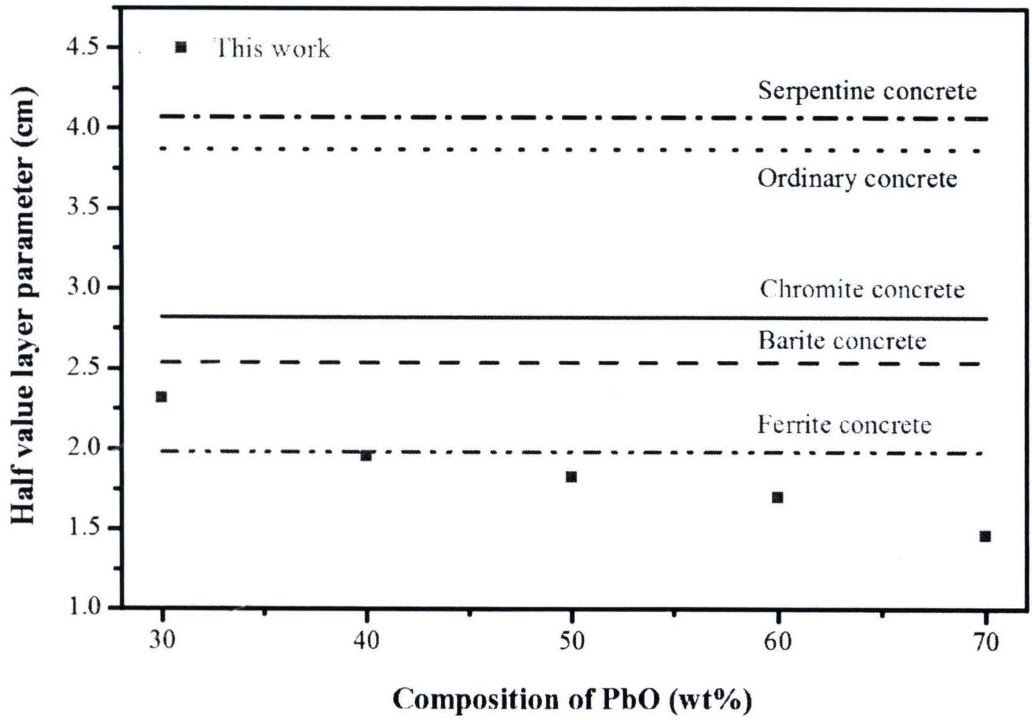


**Figure 4.18** The values of half value layer at 662 keV with different PbO content in comparison with some standard shielding concretes [2].

The results depict that the half value layer values are decreased with higher PbO concentration and the lead borate glasses are better radiation shielding materials in comparison with iron concrete. It can be concluded that $PbO$-$B_2O_3$ glass system has been found to be better than the literature concretes, indicating the potential of utilizing the research glass samples as radiation shielding.